One-dimensional ballistic channel with a triple-barrier longitudinal potential: Measurement and model

J. E. F. Frost, I. M. Castleton, C.-T. Liang, M. Pepper, D. A. Ritchie, E. H. Linfield, C. J. B. Ford, C. G. Smith, and G. A. C. Jones

Cavendish Laboratory, Madingley Road, Cambridge CB3 0HE, United Kingdom

Low-temperature measurements of the conductance of a long one-dimensional ballistic constriction with a narrow-wide-narrow-wide-narrow geometry are presented. The results are compared with a numerical calculation of the transmission probability for the longitudinal potential estimated from the lithographic dimensions, the carrier concentration, and the depth of the unpatterned two-dimensional electron gas. We find good agreement between measurement and this very simple model for particular gate-voltage conditions and when there is only one occupied one-dimensional subband. We suggest that there is electron phase coherence along the whole device at the measurement temperature of 35 mK.

The ballistic transport of electrons confined to an effectively two-dimensional layer has been studied in depth both experimentally and theoretically in recent years. One-dimensional (1D) conductance quantization[1] provides clear evidence of ballistic transport in a two-dimensional electron gas (2DEG). In the ballistic regime, where the weak-localization theory of weakly disordered systems[2] cannot be applied, there is a lack of theoretical groundwork for the calculation of the phase-coherence length and its temperature dependence. Aharonov-Bohm effects in a ring geometry[3] and in a quantum box[4] demonstrated the existence of phase-coherent electron transport in a magnetic field. Predictions of phase-coherent length resonance effects in simple split-gate devices without an applied magnetic field have not proved to be so easy to verify experimentally.[5-7]

In this paper we first review previous models of one-dimensional channels and then justify the use of our simple 1D model. Finally, we compare low-temperature conductance measurements with numerical calculations.

The split-gate device formation was by electron beam lithography and consisted of three pairs of Nichrome/ gold fingers to give a channel with a narrow-wide-narrow-wide-narrow geometry. The minimum channel width was 300 nm and the overall length was 500 nm. The conductance of the device as a function of gate voltage is shown in Fig. 1 when both gate fingers are swept together. The device resembles three split gates in series and the clear quantized ballistic conductance plateaus confirm the ballistic nature of the electron transport and the nonaddition of quantized ballistic resistance. The device geometry is shown in the inset of Fig. 1. The radius of curvature of the Schottky gate metallization in this device is greater than 10 nm, and the depth of the 2DEG is 90 nm. The mobility is 9.1×10^5 cm^2 V^{-1} s^{-1} and the sheet carrier concentration is 3×10^{11} cm^{-2} at 4.2 K. Two-terminal conductance measurements were made at 35 mK with 10-μV ac excitation and at 4.2 K with 100-μV ac excitation using standard phase-sensitive techniques.

One model of a 1D constriction comprises a channel between two semi-infinite 2DEG planes with a hard-wall confining potential: the wide-narrow-wide model.[8] This may be modified to incorporate a degree of adiabatic transport by having a linear decrease in width of channel approaching the constriction[9] or a finite radius of curvature to all the corners in the device.[10] When sharp corners or hard walls are present, length resonances are predicted with[11] and without a magnetic field[9,10,12,13] due to interference between phase-coherent components of the electron wave function reflected from the corners of rapid changes in channel width. These have previously been observed only weakly in the best cases in a simple split-gate device because it is difficult to pattern the 2DEG on a length scale comparable with the electron Fermi wavelength and have a phase coherence length greater than the device length.[6,7]

Patterning of the underlying 2DEG most closely mirrors the shape of the lithographically defined metallization at the gate voltage when depletion just occurs under the thin 100 nm width fingers. This is at a higher voltage than that needed to deplete carriers from beneath the wider metallization due to fringing effects. There-
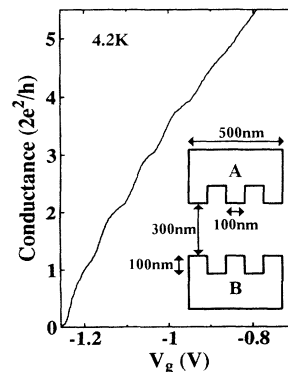

FIG. 1. Conductance in units of $2e^2/h$ as a function of gate voltage V_g at 4.2 K when the gates are swept together. The inset shows the device geometry.

49   14 078

fore, the maximum potential modulation along the channel is obtained when one side of the device is held at a constant voltage and the other is swept to reduce the device conductance. The potential modulation induced by the biased Schottky gate along the 1D channel at the depth of the 2DEG is much smaller than that at the surface. The maximum possible modulation of the potential at the 2DEG using only negative gate voltages is between ungated and fully depleted regions and has the same value as the Fermi energy, in this case 10.5 meV. In addition a screening factor of $1/(1 + a/2\pi s)$, where a is the period of the potential modulation of the 2DEG and s is the screening length (5 nm) allows us to calculate a modulation of 1.3 meV.[14]

Plateau conductances close to their predicted values suggest that there is little potential drop in the bottleneck regions. On either side of the device the 2D potential landscape varies smoothly as confirmed by the excellent agreement between measurement and calculation of split-gate conductance based on a saddle-point potential.[15] We have modeled the potential on either side of the device with a constant slope, varying between 0 and 9.5 meV over a distance of 1 μm. In the experiment, the Fermi energy E_F is constant and an increasing negative gate voltages raises the barrier height towards E_F. In the simulation, a constant barrier shape is assumed and the incident energy E is varied. We recognize that there is a change in barrier shape as the gate voltage is swept and that we can only expect qualitative agreement with the experiment. The change in barrier shape leads to thicker barriers at lower conductance, and may account for the decrease in oscillation amplitude near pinch-off.

The conductance G of the device is given by

$$G = \frac{2e^2}{h} \sum_n T_n \, , \tag{1}$$

where T_n is the total calculated transmission probability of the device for the nth 1D subband at a particular effective incident energy E.[16] The total transmission probability is calculated by breaking the potential barrier into thin strips and matching boundary conditions at each interface.[17]

The conductance was calculated for three potential profiles all with 10-meV barrier height and linearly graded potential either side of the device: A single barrier with the same length as the device (500 nm), a ten-period superlattice with the same period as the device (200 nm), and finally a triple barrier with 200-nm period. The well width was reduced from the lithographic dimension to approximate the depletion region around the gate fingers and the potential modulation was 1 meV. Figures 2(a)–2(c) show the calculated conductance for each structure and the insets the potential profile in each case.

The conductance of the device for the particular case with $V_g(A)$ held at -1.2 V and $V_g(B)$ swept is shown as the lower curve and the calculated conductance plotted as a function of incident energy E is shown as the upper curve in Fig. 3. Comparison with Fig. 2 suggests that the high-frequency oscillations at low incident energy are due to length resonance over the entire device length and
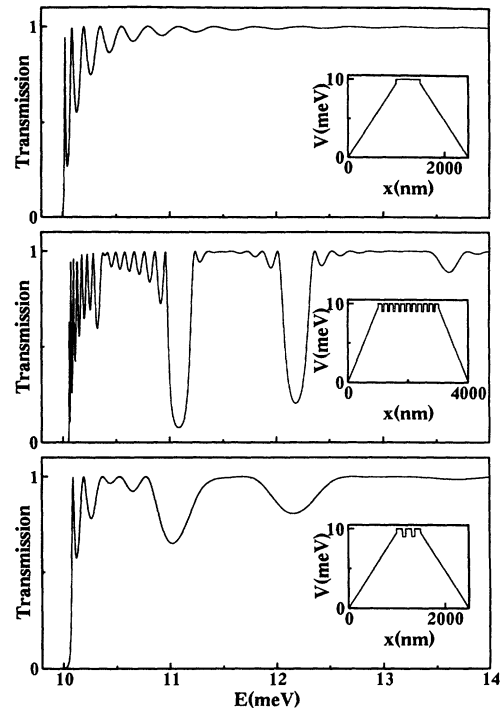

FIG. 2. The conductance calculated for three potential profiles all with barrier height 10 meV and linearly graded potential either side of the device: (a) a single barrier with the same length as the device (500 nm), (b) a ten-period superlattice with the same period as the device (200 nm), (c) a triple barrier with 200-nm period. The well width was reduced from the lithographic dimension to approximate the depletion region around the gate fingers. Inset: the potential profile in each case.

the two large dips in conductance are the beginnings of minigap formation associated with the periodicity of the device. We emphasize that the good agreement between this simple model and experiment is maintained only for particular range of gate voltage values and that more sophisticated models are required to simulate the device in
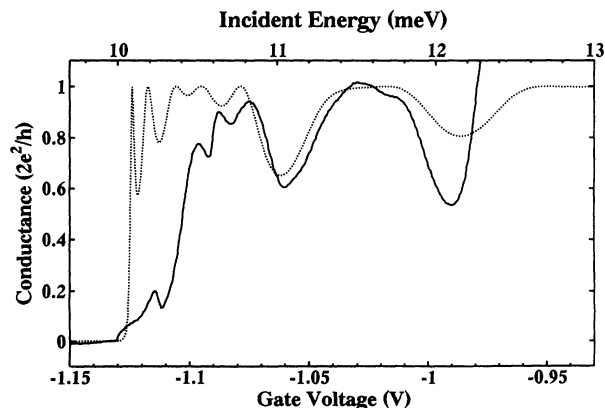

FIG. 3. Solid curve: Experimental conductance as a function of gate voltage when gate A is held at -1.2 V and gate B is swept. Dotted curve, calculated conductance obtained from the potential of Fig. 2(b) as a function of incident energy.

general, especially when there is more than one occupied 1D subband. We find a rapid reduction in amplitude of the structure observed as the temperature is increased and this also suggests that the effects are phase coherent in origin.

In summary, we have presented low-temperature conductance measurements of a one-dimensional ballistic constriction with a narrow-wide-narrow-wide-narrow geometry which are similar to theoretical predictions of phase-coherent transport along a 1D channel with modulated potential. Agreement between experiment and a simple 1D barrier model is closest when there is a single occupied one-dimensional subband.

[1] D. A. Wharam, T. J. Thornton, R. Newbury, M. Pepper, H. Ahmed, J. E. F. Frost, D. G. Hasko, D. C. Peacock, D. A. Ritchie, and G. A. C. Jones, J. Phys. C **21**, L209 (1988); B. J. van Wees, H. van Houten, C. W. J. Beenakker, J. G. Williamson, L. P. Kouwenhoven, D. van der Marel, and C. T. Foxon, Phys. Rev. Lett. **60**, 848 (1988).

[2] For a review see B. L. Altshuler and A. G. Aronov, in *Electron-Electron Interactions in Disordered Systems*, edited by A. L. Efros and M. Pollack (North-Holland, Amsterdam, 1985), p. 1; H. Fukuyama, *ibid.*, p. 155; P. A. Lee and T. V. Ramakrishnan, Rev. Mod. Phys. **57**, 287 (1985), and references therein.

[3] C. J. B. Ford, T. J. Thornton, R. Newbury, M. Pepper, H. Ahmed, D. C. Peacock, D. A. Ritchie, J. E. F. Frost, and G. A. C. Jones, Appl. Phys. Lett. **54**, 21 (1989).

[4] R. J. Brown, C. G. Smith, M. Pepper, M. J. Kelly, R. Newbury, H. Ahmed, D. G. Hasko, J. E. F. Frost, D. C. Peacock, D. A. Ritchie, and G. A. C. Jones, J. Phys. Condens. Matter **1**, 6291 (1989).

[5] L. P. Kouwenhoven, F. W. J. Hekking, B. J. van Wees, C. J. P. M. Harmans, C. E. Timmering, and C. T. Foxon, Phys. Rev. Lett. **65**, 361 (1990).

[6] C. G. Smith, M. Pepper, H. Ahmed, J. E. F. Frost, D. G. Hasko, D. C. Peacock, D. A. Ritchie, and G. A. C. Jones, J. Phys. C **21**, L893 (1988).

[7] C. G. Smith, M. Pepper, H. Ahmed, J. E. F. Frost, D. G. Hasko, R. Newbury, D. C. Peacock, D. A. Ritchie, and G. A. C. Jones, J. Phys. Condens. Matter **1**, 9035 (1989).

[8] E. Castano and G. Kirczenow, Phys. Rev. B **41**, 3874 (1990).

[9] A. Szafer and A. D. Stone, Phys. Rev. Lett. **62**, 300 (1989).

[10] Z.-L. Ji, Semicond. Sci. Technol. **8**, 1561 (1993).

[11] J. J. Palacios and C. Tejedor, Phys. Rev. B **45**, 13 725 (1992).

[12] E. Tekman and S. Ciraci, Phys. Rev. B **39**, 8772 (1989).

[13] Z.-L. Ji and K.-F. Berggren, Semicond. Sci. Technol. **6**, 63 (1991); Phys. Rev. B **45**, 6652 (1992).

[14] Y. Tokura and K. Tsubaki, Appl. Phys. Lett. **51**, 1807 (1987).

[15] N. K. Patel, J. T. Nicholls, L. Martin-Moreno, M. Pepper, J. E. F. Frost, D. A. Ritchie, and G. A. C. Jones, Phys. Rev. B **44**, 13 549 (1991).

[16] R. Landauer, IBM J. Res. Dev. **1**, 223 (1957); Philos. Mag. **21**, 683 (1970).

[17] For example, A. P. French and E. F. Taylor, *An Introduction to Quantum Physics* (Van Nostrand Reinhold, Wokingham, Berkshire, UK, 1978).